

# Early-Time Stability of Decelerating Shocks

F. W. Doss and R. P. Drake

*Department of Atmospheric, Oceanic, and Space Sciences, University of Michigan, Ann Arbor,  
MI 48105*

H. F. Robey

*Lawrence Livermore National Laboratory, Livermore, California 94550*

## ABSTRACT

We consider the decelerating shock instability of Vishniac for a finite layer of constant density. This serves both to clarify which aspects of the Vishniac instability mechanism depend on compressible effects away from the shock front and also to incorporate additional effects of finite layer thickness. This work has implications for experiments attempting to reproduce the essential physics of astrophysical shocks, in particular their minimum necessary lateral dimensions to contain all the relevant dynamics.

*Subject headings:* hydrodynamics – instabilities – shock waves

## 1. Introduction

Vishniac (1983) outlined a theory of instabilities for a system of a decelerating shock accreting mass, modeled as a thin mass shell layer possessing no internal structure. In Vishniac and Ryu (1989), the theory was expanded to include a layer of post-shock material, exponentially attenuating in density. Other work (Bertschinger (1986); Kushnir et al. (2005); among others) has described the perturbation of self-similar solutions for the post-shock flow. The present work complements these investigations, modeling the post-shock flow as a finite thickness layer of constant density and considering both compressible and incompressible post-shock states. This allows us both to more clearly understand which mechanisms depend on the compressibility of the shocked gas and which are common to any shock system undergoing deceleration.

Early in the lifetime of an impulsively driven shock, when the post-shock layer thickness is small compared to its compressible length scale, an exponential scale cannot be formed and the density profile may be closely approximated by a square wave, as a fluid everywhere of constant density. In the shock’s frame, upstream fluid is entering the shock with a speed  $V_s$  and exiting it with a speed  $U = V_s\eta$ , where  $\eta$  is the inverse compression ratio associated with the shock, including both the viscous density increase and any subsequent, localized further density increase in consequence of radiative cooling (Drake 2006).

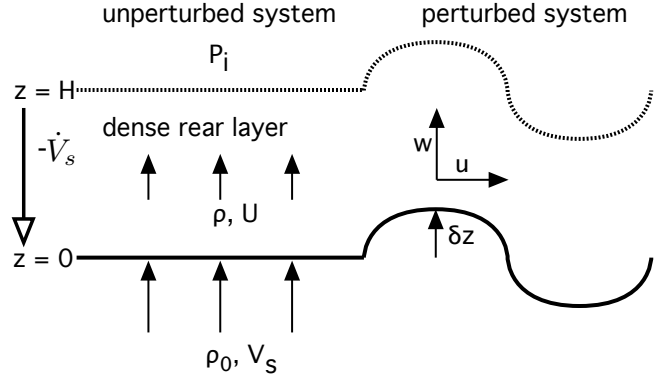


Fig. 1.— Schematic of the decelerating shock system. The solid black line is the shock, the dashed line above the dense rear layer is the rear material interface. The left-hand arrow depicts the in-frame inertial force with acceleration ( $-\dot{V}_s$ ).

We have also in mind throughout this paper experiments (Reighard et al. 2006; Bouquet et al. 2004; Bozier et al. 1986) that have been carried out to investigate radiating shock dynamics. Experiments of this type are often designed to be scaled to relevant astrophysical investigation (Remington et al. 2006). The particular experiments of Reighard et al. (2006) feature characteristic shock velocities of over 100 km/sec, shock tubes with 625  $\mu\text{m}$  diameters, and strong deceleration throughout the shocks’ lifetimes.

## 2. System of a Decelerating Shock with a Dense Downstream Layer

We consider the shock in its own, decelerating frame. The system is depicted in Figure 1. The shock is placed at  $z = 0$ , with flow entering it from the negative  $z$  direction at speed  $V_s$ , density  $\rho_0$ , and with negligible thermal pressure. Flow is exiting the shock toward positive  $z$  with speed  $U$ , density  $\rho$ , and isotropic pressure  $P$ . We will model the downstream, rear layer as a constant density region of finite, increasing thickness from  $z = 0$  to  $z = H$ . The rear surface of the dense layer will be taken to be a free interface at constant pressure. Beyond the rear layer will be taken as a region of constant thermal pressure  $P_i$ .

The native surface wave modes in the system will be right- and left-propagating waves on the two surfaces of the dense layer, leading to four modes in total. As drawn in Figure 1, the upper surface, a material discontinuity, is stable if the shock frame is decelerating and is characterized by surface gravity modes. The bottom surface, a shock at which compressibility is not suppressed, will feature propagating acoustic modes. The waves which appear in our coupled system will be modifications of these waves which appear on these surfaces in isolation. In particular, the modified acoustic waves along the shock surface will be identified as bending modes of the entire dense layer.

In order to understand the fundamental cause of the instability, we will here be considering

the fluid both ahead and behind the shock to be held at (different) densities constant in both space and time. This practice is described and defended by Hayes and Probstein (1966), who in their book “consider constant-density hypersonic flows, though we should never consider the fluid in a hypersonic flow as incompressible.” The pressure profile behind the shock is hydrostatic,  $P(z) = P_i - (H - z)\rho\dot{V}_s$ , which leads to increasing pressure at the shock front when the shock is decelerating. Perturbations to density by the waves under investigation will be discussed.

### 3. Linear Perturbations of the System

#### 3.1. Solutions Inside the Post-Shock Fluid

We begin with the inviscid fluid equations

$$\rho(\partial_t \underline{v} + \underline{v} \cdot \nabla \underline{v}) = -\nabla P - \rho\dot{V}_s \hat{z} \quad (1)$$

$$\partial_t \rho + \underline{v} \cdot \nabla \rho = -\rho \nabla \cdot \underline{v} \quad (2)$$

with total velocity  $\underline{v} = (u, 0, w + U)$  and  $P = P + \delta P$ . We will insert the perturbation  $\delta\rho$  only in the continuity equation; the coupling of  $\delta\rho$  to the frame’s acceleration will be suppressed. This allows us to ignore mode purely internal to the layer, concentrating on the overall shock and layer system. Since  $\log \rho/\rho_0 \gg \log (\rho + \delta\rho)/\rho$  for any reasonable density perturbations, we expect the dynamics of the system to be dominated by the compression at the shock. The omission of the term  $\delta\rho\dot{V}_s$  is also required for consistency with the assumption of our square wave density profile; the system will otherwise begin to evolve into an exponential atmosphere.

We first let the perturbations  $u, w, \delta P$  have time and space dependence as  $e^{nt+ikx}$ , with  $k$  real and  $n$  complex. We then linearize the x- and z- components of the momentum equation to obtain

$$(n + U\partial_z)u = -\frac{ik\delta P}{\rho} \quad (3)$$

$$(n + U\partial_z)w + w\partial_z U = -\frac{\partial_z \delta P}{\rho}. \quad (4)$$

We expressed the perturbed continuity equation in terms of perturbed pressure,

$$iku + \partial_z w = -\frac{(n + U\partial_z)\delta\rho}{\rho} = -\frac{(n + U\partial_z)\delta P}{\rho c_s^2} \quad (5)$$

where  $c_s^2 = \partial P/\partial \rho$ . We solve Equation 3 for  $\delta P$  using Equation 5, and discard terms of order  $U/c_s$  to obtain

$$\delta P = \frac{\rho}{k^2 + n^2/c_s^2} (n + U\partial_z)(-\partial_z w) \quad (6)$$

and insert that into Equation 4 to obtain a new equation for z-momentum:

$$(n + U\partial_z)w + w\partial_z U = \partial_z \left( \frac{1}{k^2 + n^2/c_s^2} (n + U\partial_z)(\partial_z w) \right) \quad (7)$$

which can now be written as a differential equation for  $w$  (taking  $U$  and  $c_s$  constant throughout the post-shock layer),

$$\left( \frac{U}{k^2 + n^2/c_s^2} \partial_z^3 + \frac{n}{k^2 + n^2/c_s^2} \partial_z^2 - U \partial_z - n \right) w = 0. \quad (8)$$

We define

$$j = \sqrt{k^2 + n^2/c_s^2}, \quad (9)$$

which describes the effective lateral wavenumber. As a wave approaches the acoustic case,  $n^2 = -k^2 c_s^2$ , the wave becomes purely longitudinal and  $j$  tends toward zero. Equation 8 has the general solution

$$w = A e^{jz} + B e^{-jz} + C e^{-nz/U}. \quad (10)$$

The system accordingly has three boundary conditions at its two interfaces: the shock and the rear surface. We note that the shock frame's acceleration  $\dot{V}_s$  does not appear in the general form of the perturbations; it will enter into the system through the boundary conditions.

The last term in Equation 10 is a consequence of the background flow  $U$  and is closely connected with structures convecting downstream with that velocity. It is instructive to consider the general solution for  $w$  in the frame of the rear surface. We introduce the coordinate  $z' = Ut - z$ . In addition, we will now write explicitly the implicit time-dependence  $e^{nt}$ . The general solution is  $w = A e^{(n+jU)t-jz'+nt} + B e^{(n-jU)t+jz'} + C e^{nz'/U}$ . We see that the third term has no time-dependence in the frame of the rear layer. In the frame of the rear surface, these flow structures are generated by perturbations in the shock surface as the shock passes some point in space, and do not evolve further. Therefore, in the frame of the shock, this term describes flow structures convecting downstream through the flow with constant velocity  $U$ . We take the shock to have been perfectly planar at the instant, some time past, at which the shock's deceleration and rear layer formation began. This allows us to explicitly set  $C = 0$  at the rear layer. We assume however that the perturbation began sufficiently early in time that our treatment using Fourier modes is sufficient, so no further information from initial conditions will be incorporated at this time.

### 3.2. Infinitely Thin Layer

We recall that the dispersion relation for the thin shell instability in its most simple form, without the effects of compression, is in Vishniac and Ryu (1989) written in the form

$$n^4 + n^2 c_s^2 k^2 - \frac{k^2 \dot{V}_s P_i}{\sigma} = 0 \quad (11)$$

where  $\sigma$  is the areal mass density of the (infinitely) thin layer, and all other variables are as we have defined them. Early work (Vishniac 1983) derived this expression for a shock of infinitesimal height but finite areal density. Such a shock, maintaining an infinitely thin layer height while continuing

to accrete mass from the incoming flow, would in our analysis be described as the limit of an infinite compression,  $\eta \rightarrow 0$ . We should expect solutions we obtain for layers of finite thickness to approach Equation 11 in this limit.

### 3.3. Free Rear Surface

We construct the boundary condition describing a free layer at  $z = H$  by applying  $\delta P = \rho(-\dot{V}_s)\delta z$  at  $z = H$ , with  $\partial_t \delta z = w$ . Using Equation 10 and our earlier expression for  $\delta P$ , Equation 6, the boundary condition becomes

$$A(n^2 - j\dot{V}_s)e^{jH} + B(-n^2 - j\dot{V}_s)e^{-jH} = 0 \quad (12)$$

where  $C$  has been explicitly set to zero as discussed above. Equation 12 is a boundary condition well known to generate surface gravity waves, when  $j = k$  and when paired with a rigid boundary condition at  $z = 0$ .

At the shock surface, we must perturb the shock momentum jump condition in the frame of the moving shock. The perturbed shock surface moving upward in Figure 1 sees a weaker incoming flow. In addition, by raising the shock surface in the hydrostatic pressure field, the effective post-shock pressure drops by an amount  $\dot{V}_s \rho \delta z$ . Our jump condition has now become

$$\rho_0(V_s - w)^2 = \rho U^2 + (P + \dot{V}_s \rho \delta z + \delta P), \quad (13a)$$

from which we obtain a boundary condition (using  $\rho_0 V_s = \rho U$ ,  $\delta z = w/n(1 - \eta)$ , and our earlier expression for  $\delta P$  in Equation 6)

$$\left( \frac{U}{k^2} \partial_z^2 + \frac{n}{k^2} \partial_z - \left( \frac{\dot{V}_s}{n(1 - \eta)} + 2U \right) \right) w \Big|_{z=0} = 0. \quad (13b)$$

The expression for  $\partial_t \delta z$  comes from conservation of mass across the shock. With density perturbations suppressed, as discussed above, we have a balance of mass flux with  $\rho_0 V_s$  entering and  $\rho U + w$  leaving the shock, with the shock moving at speed  $\partial_t \delta z$ .

$$\eta = \frac{U}{V_s} = \frac{U + w - \partial_t \delta z}{V_s - \partial_t \delta z} \quad (14a)$$

implying (with  $\partial_t = n$ )

$$w \Big|_{z=0} = (1 - \eta)n\delta z \quad (14b)$$

The third boundary condition comes from oblique shock relations. Letting  $\beta$  be the angle of the shock surface perturbation, continuity of the tangential flow requires to first order  $u \approx$

$V_s\beta = (ik)V_s\delta z$ . Applying the continuity equation of Equation 5 just downstream of the shock, and applying Equations 6 and 14b

$$\left( \partial_z - \frac{V_s k^2}{n(1-\eta)} \right) w \Big|_{z=0} = - \frac{(n + U\partial_z)\delta P}{\rho c_s^2} \quad (15a)$$

which evaluates to

$$\left( \partial_z - \frac{V_s j^2}{n(1-\eta)} \right) w \Big|_{z=0} = 0 \quad (15b)$$

Simultaneously applying these three conditions (equations 12, 13b, and 15b) on  $w$ , one demands for nonzero solutions that the determinant of the matrix of coefficients of  $A$ ,  $B$ , and  $C$ , shown collected in Equation 16, must be zero,

$$\begin{vmatrix} (n^2 - j\dot{V}_s)e^{jH} & (-n^2 - j\dot{V}_s)e^{-jH} & 0 \\ -\frac{n}{j} + U + \frac{\dot{V}_s}{n(1-\eta)} & \frac{n}{j} + U + \frac{\dot{V}_s}{n(1-\eta)} & 2U + \frac{\dot{V}_s}{n(1-\eta)} \\ \frac{1}{j} - \frac{V_s}{n(1-\eta)} & -\frac{1}{j} - \frac{V_s}{n(1-\eta)} & -\frac{n}{Uj^2} - \frac{V_s}{n(1-\eta)} \end{vmatrix} = 0 \quad (16)$$

From this one obtains, with some manipulation, the dispersion relation,

$$0 = (1-\eta)n^2 + j^2UV_s + (j\dot{V}_s + 2njU) \times \left( \frac{(n^3 + j^2UV_s) - (nj\dot{V}_s + n^2jU) \tanh jH}{(n^3 + j^2UV_s) \tanh jH - (nj\dot{V}_s + n^2jU)} \right). \quad (17)$$

We will take, as in Vishniac and Ryu (1989), the product  $UV_s$  to be equivalent to an average sound speed squared  $\langle c_s^2 \rangle$ , which we shall not henceforth distinguish from the sound speed  $c_s^2$  of material compressibility. The qualitative classification of solutions to Equation 17 depends strongly on the layer thickness  $H$ , specifically on its relation to the compressible scale height  $UV_s/|\dot{V}_s| = c_s^2/|\dot{V}_s|$ . We shall explore this dependence in what follows.

We will now investigate the range in which wavelengths of perturbations are not much shorter than  $H$ , and will approximate  $\tanh jH \approx jH$ . The existence of the critical  $H$  is easiest to see in the limit of very strong, highly compressive shocks ( $U \rightarrow 0$  while  $V_s \rightarrow \infty$  in such a way that  $UV_s = c_s^2$  and  $\dot{V}_s$  remain constant). By expanding  $j$ , we may write the dispersion relation as,

$$Tn^4 + n^2 \left( k^2 c_s^2 - \frac{\dot{V}_s^2}{c_s^2} SZ \right) - k^2 \dot{V}_s^2 S = 0 \quad (18a)$$

where we have introduced scale factors

$$T = 2 - \eta \quad (18b)$$

$$S = 1 + \frac{c_s^2/\dot{V}_s}{H} \quad (18c)$$

$$Z = 1 + \frac{2\eta(2-\eta)(S-1)}{S}. \quad (18d)$$

For strong shocks,  $T \sim (\gamma + 3)/(\gamma + 1)$ , in which any effects of strong radiation are included in  $\gamma$  as an effective polytropic index describing the total density increase at the shock (Liang and Keil 2000).  $Z$  is typically close to 1. Solutions of Equation 18, shown in Figure 2, yield instability for  $k$  in the range  $k_1 < k < k_2$ , centered around a wavenumber of maximum instability  $k_m$ , where

$$k_1 = \frac{|\dot{V}_s| \sqrt{-S}}{c_s^2} \sqrt{2T - Z - 2\sqrt{T^2 - TZ}} \quad (19a)$$

$$k_2 = \frac{|\dot{V}_s| \sqrt{-S}}{c_s^2} \sqrt{2T - Z + 2\sqrt{T^2 - TZ}} \quad (19b)$$

$$k_m = \frac{|\dot{V}_s| \sqrt{-S}}{c_s^2} \sqrt{T} \quad (19c)$$

We find that  $k_1$  and  $k_2$  are real for  $S < 0$ , requiring  $\dot{V}_s < 0$  and  $H < c_s^2/|\dot{V}_s|$ , conditions defining a decelerating shock and a layer width shorter than a scale height. The width of the region of instability  $k_2 - k_1$  may be evaluated and is greater than zero when

$$H < \frac{c_s^2}{|\dot{V}_s|} \frac{(1 - 5\eta + 2\eta^2)}{(1 - \eta)}. \quad (20)$$

This provides either an additional upper bound for layer width  $H$  or lower bound for compression  $1/\eta$ , given one of the two parameters. This requirement becomes unfulfillable if the right-hand side of Equation 20 becomes zero, necessitating a minimum compression of approximately 4.6 to produce the instability. If these conditions cannot be satisfied, the solutions become stable for all  $k$ .

For the high compression limit  $T = 2$ ,  $Z = 1$ , the critical wavenumbers take the values

$$k_1 = \frac{|\dot{V}_s| \sqrt{-S}}{c_s^2} \sqrt{3 - \sqrt{8}} \sim 0.293k_m \quad (21a)$$

$$k_2 = \frac{|\dot{V}_s| \sqrt{-S}}{c_s^2} \sqrt{3 + \sqrt{8}} \sim 1.707k_m \quad (21b)$$

$$k_m = \sqrt{2} \frac{|\dot{V}_s| \sqrt{-S}}{c_s^2} \quad (21c)$$

The solutions for growth rate at the fastest growing wavelength are

$$n_m = \pm \left( \sqrt{\frac{1}{8}} \pm i\sqrt{\frac{7}{8}} \right) \frac{|\dot{V}_s| \sqrt{-S}}{c_s} \quad (22)$$

which allow us to verify that for  $k = k_m$ ,  $jH = (k_m^2 + n_m^2/c_s^2)H$  remains small, validating our assumption.

In the opposite limit of shock strength, as  $\eta = 1$  and the shock is removed from the system,  $T = 1$  and the bending waves asymptotically approach unmodified acoustic waves at high  $k$ .

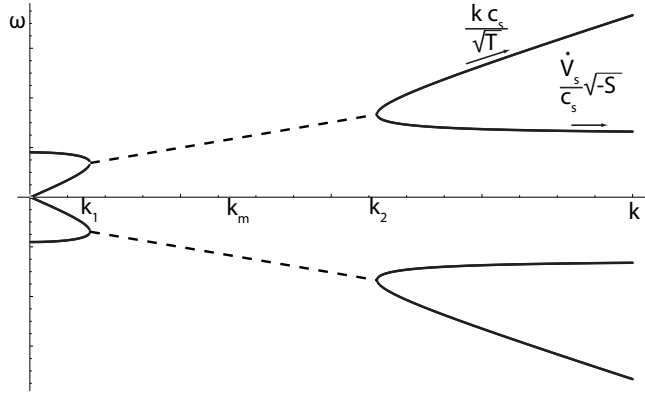


Fig. 2.— Plot showing solutions of Equation 18,  $\omega = \text{Im}(n)$  vs.  $k$ . The dashed line denotes the region of instability, where  $\text{Re}(n)$  is nonzero.

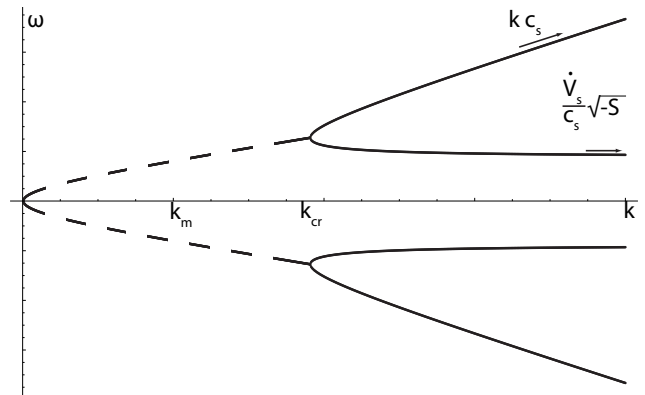


Fig. 3.— Plot showing solutions of Equation 24,  $\omega = \text{Im}(n)$  vs.  $k$ . The dashed line denotes the region of instability,  $k < k_{cr}$ , where  $\text{Re}(n)$  is nonzero.

### 3.4. Limiting Behavior of Solutions

To investigate individually the effect of various terms, we may make several further simplifying assumptions to Equation 17. We will consider both the high compression limit,  $\eta \rightarrow 0$ , as well as the limit of negligible compressibility,  $j^2 \rightarrow k^2$ . We then obtain from Equation 17 the equation

$$0 = n^2 + k^2 c_s^2 + (k \dot{V}_s + 2nkU) \times \left( \frac{(n^3 + k^2 U \dot{V}_s) - (nk \dot{V}_s + n^2 U k) \tanh kH}{(n^3 + k^2 U \dot{V}_s) \tanh jH - (nk \dot{V}_s + n^2 U k)} \right). \quad (23)$$

The  $2nUk$  term in Equation 23, which stems from the same physical source as the term discarded in Equation 6b of Vishniac and Ryu (1989), contributes to damping and shock stability in the high  $k$  limit. It was demonstrated in early work, such as that by Freeman (1955), that we expect stability for shocks separating two simple spaces of homogenous material. Accordingly, in systems with decelerating shock-bounded dense layers, as we tend to wavelengths short compared to the width of the layer, the dynamics must approach this stable limit (Vishniac 1995). The correct rate of damping is however beyond the scope of our assumptions. Ishizaki and Nishimura (1997) have shown that the acoustic modes within the shocked material, which we have suppressed, play a role in stabilizing the shock.

The limit of an indefinitely thin layer is approached, in the notation of Equation 23, by taking the limit of negligible post-shock flow  $U \rightarrow 0$ , rearranging the dispersion relation as

$$n^4 + n^2 k^2 c_s^2 - k^2 \dot{V}_s^2 \left[ 1 + \frac{c_s^2 / \dot{V}_s}{H} \right] = 0. \quad (24)$$

This shows that, in these limits, we regain the form of the Vishniac dispersion relation (Equation 11). We also see that, for  $H$  less than the scale height and  $\dot{V}_s < 0$ , the quantity in square brackets becomes negative, while this quantity is positive for large  $H$  or positive  $\dot{V}_s$ . This means that the solutions to Equation 24 have the signature of the Vishniac thin layer dispersion for an *accelerating* shock, except when  $H$  lies within a scale height for a decelerating shock,  $H < -c_s^2 / \dot{V}_s$ . Solutions when  $H$  is in that range appear as shown in Figure 3.

The region of instability is  $k < k_{cr}$ , with a maximum growth at  $k_m$ , where

$$k_{cr} = 2 \frac{|\dot{V}_s| \sqrt{-S}}{c_s^2} \quad (25a)$$

$$k_m = \frac{|\dot{V}_s| \sqrt{-S}}{c_s^2}. \quad (25b)$$

Compared with Equations 21 and Figure 2, we see that the principal result of removing the effects of compressibility is to eliminate the region of stability near  $k = 0$ . We also see that the bending modes now travel asymptotically for high  $k$  with the full speed of sound, where previously they

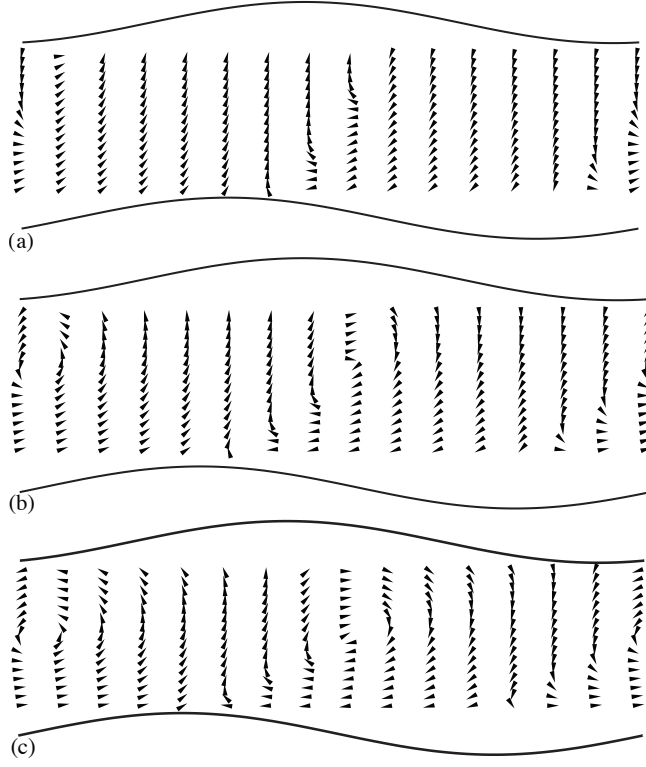


Fig. 4.— Numerical solutions of Equation 17, showing flow patterns of the perturbation  $(u, w)$  within the layer and relative phase of surface perturbations, with (a)  $H = 50 \cdot 10^{-6}$  m, (b)  $H = 110 \cdot 10^{-6}$  m, (c)  $H = 190 \cdot 10^{-6}$  m, for a shock system with  $V_s = 120 \cdot 10^3$  m/sec,  $\dot{V}_s = -5 \cdot 10^{12}$  m/sec $^2$ ,  $\eta = 0.05$ , displaying in each case a perturbation with  $k = 5210$  m $^{-1}$ .

moved at  $c_s^2/\sqrt{T}$ . Lastly, all thicknesses  $H$  less than a scale height now produce instability, rather than following the more restrictive condition in Equation 20.

We note that for  $H \ll c_s^2/|\dot{V}_s|$ , the rightmost term in Equation 24 becomes very large. As  $H$  becomes very close to zero, one perhaps expects this term to level off at the value in Equation 11; we will explore this limit below.

#### 4. Post-Shock Flow Patterns

Figure 4 shows a numerical solution of Equation 23 for a shock system with three different thicknesses. The shock system has a scale height  $c_s^2/|\dot{V}_s|$  of  $144 \cdot 10^{-6}$  m. One can see that for the very thin layer in Fig 4(a), the flow pattern is most similar to that of a surface wave. As the post-shock layer increases in thickness through Figs 4(b) and (c), the flow pattern evolves to contain vorticity features. We speculate that the transition at the scale height corresponds to a layer thickness in which a complete cell is localized.

We remark that in the numerical solution of Equation 23 we find that the shock and rear surfaces' perturbations achieve different phase. Since the fluid inside the layer is constant in density, this will lead to a corresponding perturbation of areal density of the layer that might be observed. The physical connection is therefore maintained with the theory described by Vishniac (1983), in which dynamics causing variation in areal density of the post-shock layer leads to overstability in the shock. These plots may be compared with Figures 7-10 of Bertschinger (1986), which show similar vortical structure, though without boundary phase shifting.

## 5. Further Considerations and Conclusions

### 5.1. Connections to the Infinitely Thin System

We have seen that the characteristic fourth-order nature of the Vishniac instability, as derived in Equation 17, follows from allowing perturbations on both surfaces of the post-shock layer. We note that while the Vishniac derivations contain an instability source in the product  $\dot{V}_s P_i / \sigma$ , our dispersion relation in Equation 17 contains a source term  $\dot{V}_s^2$ . This difference follows from Vishniac's assumption that the post-shock layer is thin and that the difference between thermal backing pressure and ram pressure together with geometric factors (such as spherical divergence of the shock) are the fundamental sources of the deceleration. We have instead worked with planar shocks and assumed deceleration to stem primarily from mass accumulation and energy loss from the system, for example by strong radiative cooling, and a hydrostatic distribution within the layer to be the dominant contributor to pressure variation.

Despite these differences in approach, we can in fact derive Equation 11 from Equation 24 immediately. We identify the sound speed at the shock surface with local post-shock fluid variables

$$c_s^2 = \frac{P(0)}{\rho} = \frac{P_i - \rho \dot{V}_s H}{\rho}. \quad (26)$$

We have implicitly set the polytropic index  $\gamma = 1$ , which is consistent with our assumption in Equation 24 that we are in the infinitely compressive limit  $\eta = 0$ . However, we do not expect Equation 26 to be in general consistent with our other definitions of  $c_s^2$ , except in the limit of an infinitely thin shell,  $H \rightarrow 0$ . Keeping this in mind, we see that inserting Equation 26 and  $\sigma = \rho H$  into the term in square brackets in Equation 24, one obtains Equation 11. Our derivation therefore is found to agree with the earlier results of Vishniac in the appropriate limits.

We comment on the different solutions to Equations 11, 18, and 24. The range of stable solutions when  $H < c_s^2 / |\dot{V}_s|$  but is insufficiently thin to satisfy Equation 20, is unique to the compressible, finite-shock strength solutions of Equation 17. The oscillating instability which exists when  $\dot{V}_s < 0$  and  $H$  satisfies Equation 20 is the case of interest in which collective modulation of the boundary layers results in the growth of structure. The non-oscillating instability which appears when  $\dot{V}_s > 0$  is recognized as the Rayleigh-Taylor instability of the rear layer under acceleration.

The non-oscillating solutions of Equations 18 and 24 when  $\dot{V}_s < 0$  but  $H > c_s^2/|\dot{V}_s|$  are of a different nature than the other cases. The system under perturbation was constructed by equating the pressure  $P$  immediately behind the shock with the ram pressure of the incoming material. The pressure profile then decreased hydrostatically with distance from the shock. When  $H$  exceeds a scale height, the most distant pressures obtained in this fashion become negative. The “instability” in this case is a response of the system to inconsistent initial conditions. In Vishniac’s equation, this corresponds to the case where one assigns  $\dot{V}_s, P_i < 0$ .

Compared to Equation 11, Equations 17 and 24 have the property of being written in terms of the rear layer height and variables defined locally at the compression front, with few assumptions regarding the structure throughout the layer, while Equation 11 is properly understood as dealing with quantities averaged over the layer height. This difference allows one to straightforwardly identify from Equation 24 the combination of system variables which lead to the transition at the scale height. Equation 17 features the same behavior extended to general post-shock  $U$  and finite  $\eta$ , with appropriate corrections leading to transition at a fraction of the scale height. We expect the constant density solution to be applicable within a scale height, beyond which modeling the layer as a region of constant density will not be as appropriate as an exponential or self-similar profile.

## 5.2. Experimental Observations

We conclude with some discussion of experiments featuring strongly decelerating planar shocks. Experiments which intend to reproduce this instability must feature sufficient lateral space for the growing perturbations. Very early in the experiment’s evolution, the post-shock layer thickness will be necessarily small, and we assume  $H \ll c_s^2/|\dot{V}_s|$ . We see from the results of the proceeding compressible analysis (Equations 21 and 22) that to allow maximum growth one must afford the experiment lateral dimensions  $\lambda > 2\pi c_s \sqrt{H/2|\dot{V}_s|}$ , where  $H$  is a characteristic or average layer thickness of the system. The evolution will occur within a growth time scale  $t = \sqrt{8H/|\dot{V}_s|}$ . Conversely, if one wishes to eliminate entirely this instability one should construct an experiment with lateral dimensions  $\lambda \lesssim 2.6 c_s \sqrt{H/|\dot{V}_s|}$ . For the experiments discussed above by Reighard et al. (2006), the values of preferred minimum distance and time are approximately 400 - 500  $\mu\text{m}$  and 9 - 13 ns, conditions which are achievable by the reported experiment.

This research was supported by the DOE NNSA under the Predictive Science Academic Alliance Program by grant DE-FC52-08NA28616, the Stewardship Sciences Academic Alliances program by grant DE-FG52-04NA00064, under the National Laser User Facility by grant DE-FG03-00SF22021, and by the Stewardship Science Graduate Fellowship program.

## REFERENCES

E. T. Vishniac, ApJ **274**, 152 (1983).

E. T. Vishniac and D. Ryu, ApJ **337**, 917 (1989).

E. Bertschinger, ApJ **304**, 154 (1986).

D. Kushnir, E. Waxman, and D. Shvarts, ApJ **634**, 407 (2005).

R. P. Drake, *High-Energy-Density Physics* (Springer, 2006).

A. B. Reighard, R. P. Drake, K. K. Dannenberg, D. J. Kremer, M. Grosskopf, E. C. Harding, D. R. Leibbrandt, S. G. Glendinning, T. S. Perry, B. A. Remington, et al., Phys. Plasmas **13**, 082901 (2006).

S. Bouquet, C. Stéhlé, M. Koenig, J.-P. Chièze, A. Benuzzi-Mounaix, D. Batani, S. Leygnac, X. Fleury, H. Merdji, C. Michaut, et al., Phys. Rev. Lett. **92**, 225001 (2004).

J. C. Bozier, G. Thiell, J. P. Le Breton, S. Azra, M. Decroisette, and D. Schirrmann, Phys. Rev. Lett. **57**, 1304 (1986).

B. A. Remington, R. P. Drake, and D. D. Ryutov, Reviews of Modern Physics **78**, 755 (2006).

W. Hayes and R. Probstein, *Hypersonic Flow Theory* (Academic Press, 1966).

Edison Liang and Katherine Keilty, ApJ **533**, 890 (2000).

N. C. Freeman, Royal Society of London Proceedings Series A **228**, 341 (1955).

E. T. Vishniac, New York Academy Sciences Annals **773**, 70 (1995).

R. Ishizaki and K. Nishimura, Phys. Rev. Lett. **78**, 1920 (1997).